CHEMISTRY
A EUROPEAN JOURNAL

ChemPubSoc
Europe

DOI: 10.1002/chem.201103631

Click Ionic Liquids: A Family of Promising Tunable Solvents and Application in Suzuki–Miyaura Cross-Coupling

Liuyi Li, Jinyun Wang, Tao Wu, and Ruihu Wang*[a]

Abstract: A series of click ionic salts **4a–4n** was prepared through click reaction of organic azides with alkyne-functionalized imidazolium or 2-methylimidazolium salts, followed by metathesis with lithium bis(trifluoromethanesulfonyl)amide or potassium hexafluorophosphate. All salts were characterized by IR, NMR, TGA, and DSC, and most of them can be classified as ionic liquids. Their steric and electronic properties can be easily tuned and modified through variation of the aromatic or aliphatic substituents at the imidazolium and/or triazolyl rings. The effect of anions and substituents at the two rings on the physicochemical properties was investigated. The charge and orbital distributions based on the optimized structures of cations in the salts were calculated. Reaction of **4a** with $PdCl_2$ produced mononuclear click complex **4a-Pd**, the structure of which was confirmed by single-crystal X-ray diffraction analysis. Suzuki–Miyaura cross-coupling shows good catalytic stability and high recyclability in the presence of $PdCl_2$ in **4a**. TEM and XPS analyses show formation of palladium nanoparticles after the reaction. The palladium NPs in **4a** are immobilized by the synergetic effect of coordination and electrostatic interactions with 1,2,3-triazolyl and imidazolium, respectively.

Keywords: click chemistry · cross-coupling · ionic liquids · nanoparticles · palladium

Introduction

Transition metal catalyzed cross-coupling reactions have provided an efficient and versatile tool for connection of two fragments by C–C bond formation in organic synthesis.[1–3] Metal nanoparticles (NPs) are known to be more reactive than their particulate metal counterparts in catalytic reactions.[3–7] As NPs are thermodynamically unstable, protective agents are usually used to prevent their aggregation, for example by addition of stabilizers[4] or by supporting NPs on solid materials.[5] Immobilization of NPs has been achieved by coordination, steric, and electrostatic interactions or their synergetic effects. However, soluble metal NPs have many advantages over heterogeneously supported metal NPs that are restricted by support surfaces, such as controllable size, more degrees of free rotation, and more active sites accessible to reactants,. Moreover, the optimum balance between activity and stability of soluble NPs is easily tuned through careful choice and modification of stabilizers.[6–8] Although soluble NPs show very high catalytic activity in organic, aqueous, polyethylene glycol, and even fluorous media,[7,8] difficulties in separation and reuse limit their practical applications. Therefore, much research has been devoted to a judicious combination of stabilizers and reaction media to facilitate separation and recycling of soluble NPs.

Imidazolium-based ionic liquids (ILs) have been extensively used as alternative reaction media in catalytic reactions.[9] It is now well established that ILs can stabilize metal NPs by electrostatic interaction. Palladium NPs with different topologies have been prepared in various ILs, and their catalytic activities in ILs have been investigated.[10] Nevertheless, the tendency of palladium NPs in simple imidazolium-based ILs to aggregate after catalytic reactions results in decreased recyclability and loss of catalytic activity. Recently, thiol-,[11] nitrile-,[12] pyrazolyl-,[13] pyridyl-,[14] and imidazolyl-functionalized[15] ILs have been used as both reaction media and stabilizers of palladium NPs. Stable catalyst systems are achieved by the synergistic effect of coordination and electrostatic interactions. In general, ILs that coordinate more strongly to palladium NPs give more stable catalyst systems, but they tend to prevent access of substrates to the active centers. On the contrary, weak coordination ability of the ILs to palladium NPs can result in high catalytic activity, but aggregation of NPs may occur. Both cases can ultimately lead to less effective catalysts.[16] To obtain an optimum balance between stability and reactivity, flexible variation and modification of ILs are crucial, since their steric and electrical characters as well as coordination ability to palladium have an important effect on physicochemical properties of NPs. However, most modifications of the ILs focused on the

[a] L. Li, J. Wang, T. Wu, Prof. R. Wang
State Key Laboratory of Structural Chemistry
Fujian Institute of Research on the Structure of Matter and
Key Laboratory of Coal to Ethylene Glycol
and Its Related Technology
Chinese Academy of Science
Fuzhou, Fujian, 350002 (P.R. China)
E-mail: ruihu@fjirsm.ac.cn

Supporting information for this article is available on the WWW under http://dx.doi.org/10.1002/chem.201103631.

substituents of the imidazolium group,[11–15] and tuning of the coordinating group has seldom been explored.

Click reaction between azides and terminal alkynes to give 1,4-disubstituted 1,2,3-triazoles has attracted much attention, since the reaction usually shows high modularity, wide group tolerance, high yield, and high regioselectivity.[17] Utilization of 1,2,3-triazolyl as a stable linkage for the connection of two chemical/biological components,[18] as an adaptive ligand for the binding of metal ions,[19–22] and as a stabilizer of palladium NPs[20] has been realized. The classes of clickphine,[21] clickphos,[22] clickcarbene,[23]and click phosphine-containing pincer ligands[24] were also synthesized. Inspired by flexible adjustability and high catalytic efficacy of the palladium complexes, we envisioned that ILs resulting from the combination of the 1,2,3-triazolyl and imidazolium might be attractive, because highly modular synthetic accessibility of each or both of them would enable facile tuning of their steric and electronic properties for immobilization of metal NPs. In addition, high group tolerance in the click reaction makes it feasible to synthesize novel ILs for specific applications. As a continuation of our research on environmentally friendly reaction media,[25] herein, we report the synthesis and characterization of a family of imidazolium-based click ILs, the steric and electronic properties of which can be readily tuned and modified through variation of substituents at the imidazolium and/or triazolyl rings. The ILs were used as solvents and stabilizers of palladium NPs, and their application in Suzuki–Miyaura cross-coupling reaction was preliminarily evaluated.

Results and Discussion

The synthetic pathway for click ionic salts **4a**–**4n** is depicted in Scheme 1 and Table 1. Alkyne-functionalized 2-methylimidazolium (**2a**, **2c**) and imidazolium (**2b**, **2d**, **2e**) salts were readily prepared by quaternization of **1** with propargyl bromide in boiling toluene. Click reactions between **2a**–**2e** and organic azides in the presence of copper sulfate and sodium ascorbate gave triazolyl-functionalized ionic salts **3a**–**3i**. Subsequent metathesis with lithium bis(trifluoromethanesulfonyl)amide ($LiNTf_2$) or potassium hexafluorophosphate (KPF_6) resulted in the formation of click ionic salts **4a**–**4n**. Compound **4n** with mesitylimidazolium parent ring can be classified as a tunable aryl-alkyl IL and fulfils the standard for next-generation ILs.[26] The steric and electronic properties of the click ionic salts can be flexibly modified by variation of substituents (R′, R″, and R‴) at the imidazolium and/or triazolyl rings. Though only fourteen salts are presented herein, the powerful methodology provides a facile route for the synthesis of a variety of ionic salts and flexible structural tuning by using readily available azides and alkyne-quaternized aryl imidazolium or alkyl imidazolium compounds.

All salts are stable in air and water. They were characterized by NMR and IR spectroscopy and elemental analysis.

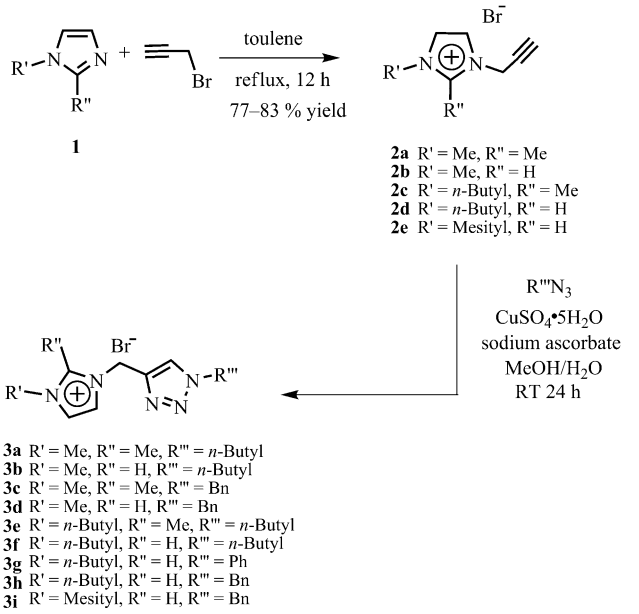

Scheme 1. Synthesis of click ionic salts **3a**–**3i**.

Table 1. Thermal properties of click ionic salts **4a**–**4n**.

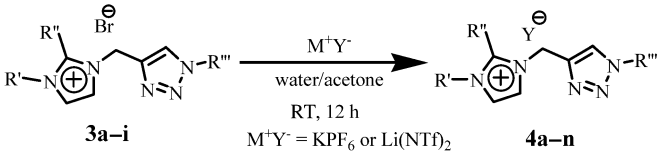

Compound	R′	R″	R‴	Y^-	T_m [°C][a]	T_d [°C][b]
4a	Me	Me	*n*Bu	PF_6^-	74	327
4b	Me	H	*n*Bu	PF_6^-	−39[c]	319
4c	Me	Me	*n*Bu	NTf_2^-	−53[c]	349
4d	Me	H	*n*Bu	NTf_2^-	−59[c]	333
4e	Me	Me	Bn	PF_6^-	114	328
4f	Me	Me	Bn	NTf_2^-	−30[c]	360
4g	Me	H	Bn	PF_6^-	85	328
4h	*n*Bu	H	Bn	PF_6^-	87	324
4i	*n*Bu	H	Bn	NTf_2^-	−40[c]	340
4j	*n*Bu	H	Ph	PF_6^-	113	302
4k	*n*Bu	H	Ph	NTf_2^-	−43[c]	322
4l	*n*Bu	H	*n*Bu	PF_6^-	−48[c]	312
4m	*n*Bu	Me	*n*Bu	PF_6^-	−27[c]	316
4n	Mes	H	Bn	PF_6^-	48	312

[a] Melting point. [b] Thermal degradation. [c] Glass transition temperature.

In their ^{1}H NMR spectra, the typical signal for the proton of the triazolyl ring is in the range of 8.06–8.12 ppm, which is upshifted in comparison with the respective precursors **3a**–**3i** (8.22–8.34 ppm). As expected, the carbon resonance for triazolyl CH in the ^{13}C NMR spectrum is observed at 124.0 ± 0.5 ppm, which is upshifted relative to the other C atoms of the triazolyl ring (140.0 ± 0.5 ppm). The chemical shift of the methylene protons between imidazolium and triazolyl rings in **4a**–**4n** is observed as a singlet in the ^{1}H NMR spectra and falls in the range from 5.54 to 5.64 ppm, which is higher than those between triazolyl and phenyl rings in

4e–**4i** and **4n** (5.46–5.54 ppm). The proton in the 2-position of the imidazolium ring in **4b**, **4d, 4j**–**4l**, and **4n** has a chemical shift of 9.00±0.20 ppm, and is thus unaffected by substitution at the imidazolium and triazolyl rings.

Phase-transition temperatures (melting points or glass transition temperatures) were determined by differential scanning calorimetry (DSC). The relationship between phase-transition temperatures and the structures of **4a**–**4n** is clearly observed in Table 1. The anion has a major influence on the melting point. For salts with the same cation, when the anion is changed from PF_6^- in **4a**, **4b**, **4e**, **4h**, and **4j** to NTf_2^- in **4c**, **4d**, **4f**, **4i**, and **4k**, the respective phase-transition temperature is markedly decreased. All of the NTf_2^- salts can be classified as room-temperature ILs. However, the phase-transition temperatures of PF_6^- salts are over 25 °C, except for **4b** and **4l**, which are liquids at room temperature, and **4e** and **4j**, which have melting points above 100 °C, outside of the temperature range of ILs, and thus can not be classified as ILs. The length and flexibility of substituents at the imidazolium and triazolyl rings also affect the phase-transition temperatures of the salts. For the imidazolium-based PF_6^- salts, the effect of *N*-substituents of the triazolyl ring on melting points is in the following order: 113 (Ph, **4j**) > 87 (Bn, **4h**) > −48 °C (*n*-butyl, **4l**). For the imidazolium-based and 2-methylimidazolium-based NTf_2^- salts, when *N*-substituents at the triazolyl ring are changed from Bn to Ph and from Bn to *n*-butyl, the phase-transition temperatures vary from −40 (**4i**) to −43 °C (**4k**) and from −30 (**4f**) to −53 °C (**4c**), respectively. As expected, when *N*-substituents at the imidazolium and 2-methylimidazolium rings are changed from methyl to *n*-butyl, the phase-transition temperatures varied from 74 (**4a**) to −27 °C (**4m**) and from −39 (**4b**) to −48 °C (**4l**), respectively.

Thermal stabilities of **4a**–**4n** were determined by thermogravimetric analysis (TGA). Variation of *N*-substituents at the triazolyl and imidazolium parent rings has no apparent effect on their decomposition temperatures, but anions show a remarkable influence. The NTf_2^- salts are more thermally stable than the analogous PF_6^- salts; their decomposition temperatures are in the ranges of 322–360 °C and 302–328 °C, respectively, which are comparable with those of reported similar coordination ILs.[13a] However, thermal decomposition of **4a-Pd** occurs at 250 °C, which is much lower than for **4a** (327 °C).

To gain better insight into the click ionic salts, natural bond orbital (NBO) and molecular orbital analyses based on the optimized structures of the cations in **4a**–**4n** (B3LYP/6-311g*) were performed with Gaussian 03.[27] The charge distributions of the nine cations are shown in Table 2 and Figure S1 of the Supporting Information. C1 and C5 carry the positive charge, while the rest of carbon and nitrogen atoms have negative charge in the frameworks of cations **1**–**9**. The positive charge of C1 in 2-methylimidazolium-based cations (**1**, **2**, and **5**) is much higher than that of imidazolium-based cations. However, a slightly more negative charge of the methylene bridge (C4) in 2-methylimdazolium-based cations (**1**, **2**, and **5**) is observed when compared with analogous imidazolium-based cations. Among the nitrogen atoms of the triazolyl ring, N3 carries the most negative charge and thus should preferably coordinate to metal ions, which was further confirmed by the X-ray crystal structure of **4a-Pd** (see below). The charge distribution of N5 in the triazolyl ring is less negative when its substituents are changed from *n*-butyl (**1**, **3**, **5**, and **6)** to benzyl (**2**, **4**, **7**, and **9**) or phenyl (**8**). The triazolyl group carries the negative charge, while the rest of groups, such as *N*-substituents, imidazolium, and 2-methylimidazolium, have positive charge. The triazolyl ring and phenyl substituent in **8** exhibit the most negative charge and the lowest positive charge, respectively, which are ascribed to the stronger conjugative effect between triazolyl and phenyl rings. Similar results are observed for aryl-substituted imidazolium groups.

The imidazolium and mesityl substituents in cation **9** have the lowest and highest positive charge, respectively, owing to the delocalization of the positive charge between mesityl and imidazolium groups, and thus the charge of N1 in **9** is more negative than analogues in other cations. When *N*-substituents at the imidazolium ring are changed from Me to *n*-butyl to mesityl while keeping the other groups unchanged,

Table 2. Charge distributions of atoms and groups in the cations of **4a**–**4n**.

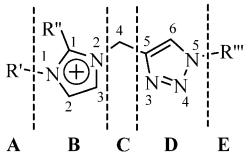

Cation 1 R' = Me, R'' = Me, R''' = *n*-Butyl
Cation 2 R' = Me, R'' = Me, R''' = Bn
Cation 3 R' = Me, R'' = H, R''' = *n*-Butyl
Cation 4 R' = Me, R'' = H, R''' = Bn
Cation 5 R' = *n*-Butyl, R'' = Me, R'''= *n*-Butyl
Cation 6 R' = *n*-Butyl, R'' = H, R'''= *n*-Butyl
Cation 7 R' = *n*-Butyl, R'' = H, R'''= Bn
Cation 8 R' = *n*-Butyl, R'' = H, R'''= Ph
Cation 9 R' = Mesityl, R'' = H, R''' = Bn

Atom or group	Cation **1**	Cation **2**	Cation **3**	Cation **4**	Cation **5**	Cation **6**	Cation **7**	Cation **8**	Cation **9**
C1	0.482	0.482	0.286	0.287	0.486	0.288	0.288	0.289	0.296
C2	−0.017	−0.017	−0.014	−0.015	−0.022	−0.016	−0.156	−0.015	−0.006
C3	−0.010	−0.010	−0.002	−0.002	−0.010	−0.006	−0.006	−0.005	−0.014
C4	−0.189	−0.189	−0.185	−0.185	−0.189	−0.185	−0.185	−0.185	−0.185
C5	0.036	0.038	0.032	0.035	0.037	0.034	0.036	0.038	0.037
C6	−0.025	−0.022	−0.023	−0.019	−0.026	−0.024	−0.021	−0.019	−0.021
N1	−0.361	−0.361	−0.348	−0.348	−0.367	−0.354	−0.354	−0.354	−0.377
N2	−0.359	−0.358	−0.346	−0.346	−0.367	−0.351	−0.350	−0.351	−0.350
N3	−0.289	−0.288	−0.291	−0.290	−0.289	−0.290	−0.289	−0.281	−0.287
N4	−0.040	−0.040	−0.039	−0.039	−0.041	−0.040	−0.040	−0.035	−0.041
N5	−0.180	−0.187	−0.180	−0.186	−0.181	−0.180	−0.187	−0.186	−0.187
A	0.315	0.315	0.324	0.324	0.340	0.347	0.347	0.346	0.362
B	0.355	0.356	0.338	0.339	0.333	0.319	0.319	0.321	0.310
C	0.278	0.279	0.284	0.284	0.277	0.282	0.282	0.283	0.282
D	−0.267	−0.260	−0.267	−0.260	−0.268	−0.267	−0.261	−0.246	−0.260
E	0.319	0.311	0.321	0.313	0.318	0.319	0.311	0.294	0.310

the positive charge of imidazolium parent ring follows the trend Me (**4**) > *n*-butyl (**7**) > mesityl(**9**), and the positive charge of the *N*-substituents the reverse trend.

The HOMOs and LUMOs in cations **1**–**9** were also explored. As shown in Figure S2 (Supporting Information), the *N*-benzyl substituent at the triazolyl ring occupies most of HOMO in the cations **2**, **4**, **7**, and **9**. However, when *N*-substituents are Me or *n*-butyl in cations **1**, **3**, **5**, and **6**, HOMOs are mainly occupied by the triazolyl ring. Interestingly, the HOMO is shared by triazolyl and phenyl substituents in cation **8** owing to their conjugative effect. the LUMO in cations **1**–**9** is occupied by imidazolium or 2-methylimidazolium. The LUMO is not shared by the mesityl substituent in cation **9** despite the strong delocalization effect between the groups.

The coordination ability of the click ionic salts with palladium(II) was also briefly studied. Single crystals of **4a-Pd** were obtained by slow evaporation of acetone solution of **4a** and palladium(II) chloride. The crystal structure of **4a-Pd** was determined by single-crystal X-ray diffraction. As shown in Figure 1, the palladium(II) center is in a distorted

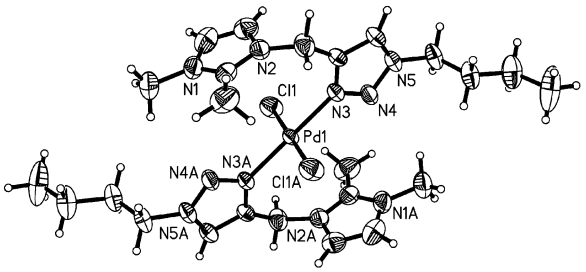

Figure 1. Crystal structure of **4a-Pd** with thermal ellipsoids at 50% probability; PF_6^- was omitted for clarity.

square-planar geometry and is coordinated by two *trans* triazolyl nitrogen atoms from **4a** and two *trans* chloride ions. The *cis* angles range from 88.55(7) to 91.45(7)°, and the Pd–N and Pd–Cl distances are 2.015(2) and 2.2914(9) Å, respectively. Salt **4a** serves as a monodentate ligand, and the dihedral angle between imidazolium and triazolyl rings is 80.5°. There are no other short contacts or significant weak interactions between adjacent cations.

Coordination ILs can serve as promising reaction media and ligands of metal ions in catalytic reactions.[12–15] To evaluate catalytic stability and recyclability of palladium in the click ILs, Suzuki–Miyaura cross-coupling reactions between aryl boronic acids and aryl iodides were tested. As shown in Table 3, treatment of phenylboronic acid with iodobenzene in the presence of K_2CO_3 and 2.0 mol% $PdCl_2$ in **4a** gave rise to biphenyl in quantitative GC yield. The product was easily separated from the catalytic solution by simple extraction with diethyl ether, and the resulting solution was washed with water to remove inorganic salts and then dried under vacuum for the next cycle. When the catalytic solution was used seven times in the cross-coupling reaction

Table 3. Recyclable Suzuki–Miyaura cross-coupling reaction between aryl halide and aryl boronic acid.[a]

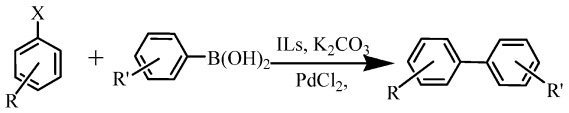

Entry	Run	X	R	R′	Yield[b]
1	1	I	H	H	100
2	2	I	H	H	100
3	3	I	H	H	100
4	4	I	H	H	100
5	5	I	H	H	100
6	6	I	H	H	100
7	7	I	H	H	99
8	1	Br	4-CN	H	100 (96)
9	2	I	4-F	H	100 (100)
10	3	I	H	H	100 (100)
11	4	I	4-NO_2	H	96 (94)
12	1	I	H	4-CH_3CO	99 (99)
13	2	I	H	4-CH_3CO	99 (98)
14	3	I	H	3-Me	98 (89)
15	4	I	H	4-MeO	95 (73)
16	5	I	H	2-Me	98 (93)

[a] All reactions were carried out with 0.5 mmol of aryl halide, 0.6 mmol of aryl boronic acid, 1.0 mmol of K_2CO_3, 0.5 mL of H_2O, 2 mol% of $PdCl_2$, and 2.0 g of **4a** at 100 °C for 5 h. [b] GC yield (yield of isolated product).

under identical conditions, no obvious loss of catalytic activity was observed (Table 3, entries 1–7), and this suggests that palladium species are effectively immobilized in the click ILs during reaction and product separation. Apparently, coordination of triazolyl group to palladium species and electrostatic interaction of 2-methylimidazolium synergistically prevent decomposition of the catalysts. To further test the scope and recyclability of the catalytic system, cross-coupling reactions between aryl halides and phenylboronic acid were performed by using similar protocols, and the corresponding target products were isolated in high yields (Table 3, entries 8–11). Cross-coupling reactions between iodobenzene and the other aryl boronic acids were also examined (Table 3, entries 12–16). The corresponding biaryl products were isolated in excellent yields, whereby the electronic and steric nature of the boronic acids had no obvious effect on the cross-coupling reactions. It is noteworthy that the catalytic solution could be used five times with different reactants without apparent loss of catalytic activity.

Active palladium NPs are usually involved in palladium-catalyzed cross-coupling reactions. To identify the catalytically active species in the Suzuki–Miyaura cross-coupling reaction, the reaction between iodobenzene and phenylboronic acid in the presence of $PdCl_2$ and **4a** was selected as a model reaction. After the first run of the reaction, ethanol was added to the catalytic solution, and a black powder was isolated by centrifugation (NPs, designated Pd-Suzuki). The isolated powder was analyzed by TEM and X-ray photoelectron spectroscopy (XPS). The TEM images show the formation of palladium NPs with a mean diameter of 3.77 ± 0.71 nm (Figure 2). The palladium NPs are stable in **4a** and no precipitate is observed for months. The XPS spectrum

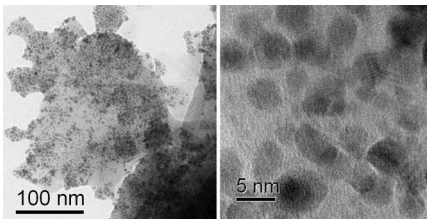

Figure 2. TEM image of Pd-Suzuki.

showed that the Pd 3d region is divided into two spin–orbital pairs with $3d_{5/2}$ binding energies of 335.59 and 334.34 eV (Figure 3). The binding-energy peaks at 334.34 (Pd $3d_{5/2}$) and 339.59 eV (Pd $3d_{3/2}$) can be assigned as Pd^0 species, while the peak at 335.59 eV indicates the presence of Pd^{II} in the palladium particles, which may be attributed to partial oxidation of Pd^0 after exposure to air.[28]

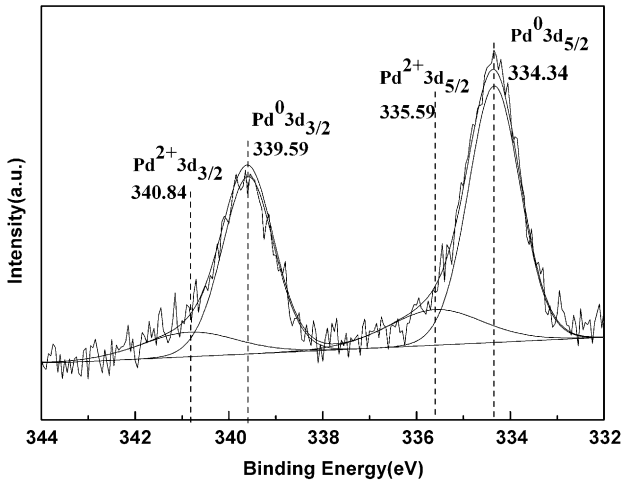

Figure 3. XPS of Pd-Suzuki.

For comparison, palladium NPs were also prepared by reducing Pd^{II} with $NaBH_4$ in **4a** (Pd-$NaBH_4$). The TEM images of Pd-$NaBH_4$ (Figure 4) indicate the presence of palladium NPs with a mean diameter of 3.59 ± 0.72 nm, which is close to that of Pd-Suzuki. The palladium NPs in **4a** are immobilized by the synergetic effect of coordination and electrostatic interactions of 1,2,3-triazolyl and 2-methylimidazolium, respectively. If the triazolyl group in **4a** coordinates to the surface of palladium NPs to prevent their agglomeration, then the repulsive action of the positive charge of imidazolium group will result in uniform distribution and small size of the NPs.[12a] The XRD pattern of Pd-$NaBH_4$ further confirms the presence of crystalline Pd^0 (Figure 5).

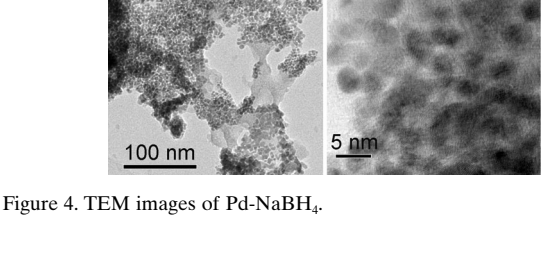

Figure 4. TEM images of Pd-$NaBH_4$.

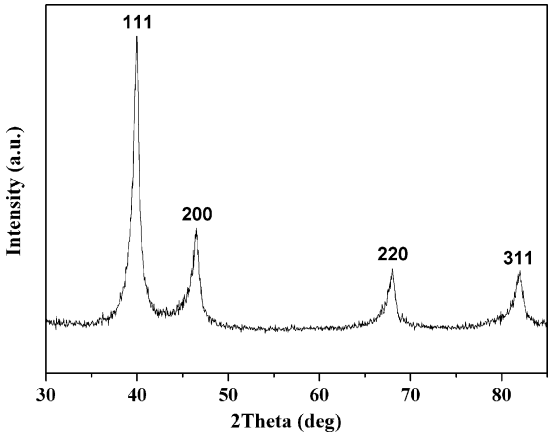

Figure 5. XRD of Pd-$NaBH_4$; the peaks are labeled with *hkl* of planes for the corresponding Bragg angles.

The Bragg reflections at 39.9808, 46.5008, 67.5998 and 81.6008° correspond to (111), (200), (220), and (311) lattice planes of fcc Pd^0 with a unit cell parameter of $\alpha = 3.89$ Å.[29]

As shown in Figure 6a, two set of distinct signals are observed for Pd 3d XPS of Pd-$NaBH_4$, indicating the presence of two types of the surface-bound palladium species. The peaks at 335.11 (Pd $3d_{5/2}$) and 340.36 eV (Pd $3d_{3/2}$) are assigned to Pd^0 species. The Pd $3d_{5/2}$ and Pd $3d_{3/2}$ binding energies of Pd-$NaBH_4$ are 0.77 and 0.52 eV higher than the respective values of Pd-Suzuki. The other peaks at 336.11 and 341.36 eV belong to Pd^{II} species. The peak area of Pd^{II} species is much smaller than that of Pd^0 species. The N 1s spectra of **4a** and Pd-$NaBH_4$ were also measured (Figure 6b). The peaks of **4a** at 398.4 and 399.8 eV are consistent with the literature data for the N 1s binding energy of imidazolium cation[30] and 1,2,3-triazolyl,[31] respectively. The N 1s binding energies of Pd-$NaBH_4$ of 399.3 and 400.4 eV are slightly higher than those of **4a**, which is ascribed to N atoms of **4a** in Pd-$NaBH_4$ being in an electron-poor state due to the coordination of **4a** with Pd species.

Conclusion

A series of imidazolium-based click ionic salts have been easily prepared, and their steric and electronic properties can be flexibly tuned through variation of the substituents at the imidazolium and/or 1,2,3-triazolyl rings. Natural bond orbital analyses indicate that their charge and orbital distributions differ quite widely due to the different substituents at the imidazolium or 1,2,3-triazolyl ring. The click salts can be used as both ligands of palladium(II) and solvents in

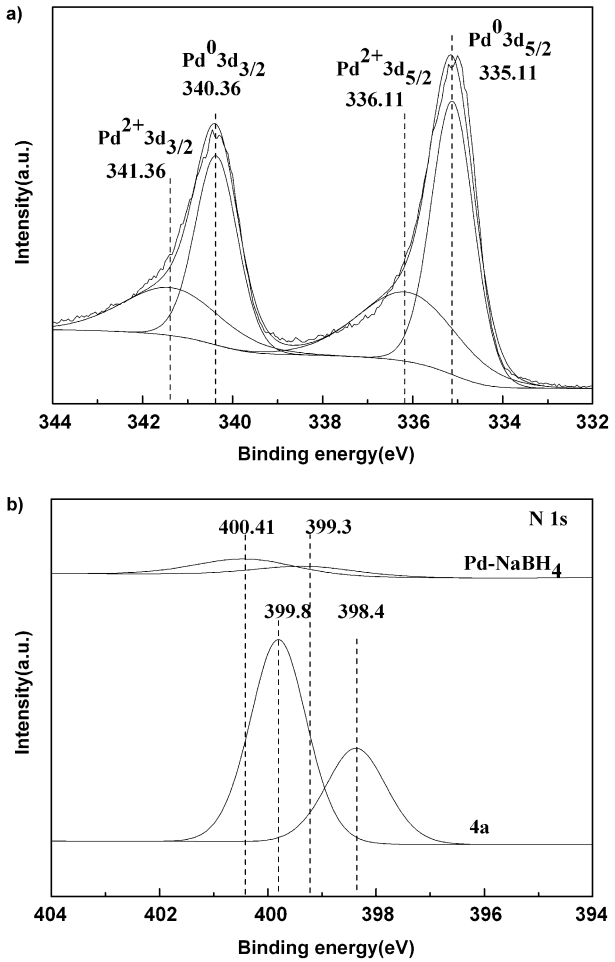

Figure 6. a) XPS of Pd-$NaBH_4$. b) N 1s XPS of **4a** (top) and Pd-$NaBH_4$ (bottom).

Suzuki–Miyaura cross-coupling. TEM and XPS analyses show formation of palladium NPs after the catalytic reaction. The click ILs serve as efficient protective agents of palladium NPs. The NPs are immobilized by the synergetic effect of coordination and electrostatic interactions of 1,2,3-triazolyl and imidazolium, respectively, in the click salts, which results in small NPs and good stability of catalysts during reaction and separation. In summary, this study provides a powerful methodology for the synthesis and modification of functional ILs, especially functionalized new-generation aryl-alkyl ILs. Further exploration of the relationship between NPs structures and subsitutents of the click ILs, as well as extension of their application, is in progress.

Experimental Section

General methods: All chemicals were obtained from commercial suppliers and were used without further purification. Standard Schlenk techniques were used for performing air- and moisture-sensitive reactions under nitrogen atmosphere. ^1H, ^{13}C, ^{31}P, and ^{19}F NMR spectra were recorded on a Bruker Biospin Avance III spectrometer at 400, 100, 162, and 376 MHz, respectively. Chemical shifts are reported in ppm relative to TMS. The IR spectra were recorded on KBr pellets by using PerkinElmer Instruments. Thermogravimetric analysis (TGA) was carried out on NETZSCH STA 449C by heating samples at 10 °C min^{-1} from room temperature to 700 °C under nitrogen atmosphere. Differential scanning calorimetry (DSC) was performed in a calorimeter equipped with an autocool accessory. The following procedures were used for each sample: cooling from 40 °C to −170 °C and then heating to 200 °C at 10 °C min^{-1}. The transition temperature was taken as peak maximum. Onset of decomposition was taken when the abnormal section of the plot began. XPS measurements were performed on a Thermo ESCALAB 250 spectrometer, with nonmonochromatic $Al_{K\alpha}$ radiation as primary excitation source. The binding energies were calibrated with the C 1s level of adventitious carbon (284.8 eV) as internal standard reference. XRD patterns were recorded in the range of $2\theta = 5$–$80°$ by a desktop X-ray diffractometer (RIGAKU-Miniflex II) with $Cu_{K\alpha}$ radiation ($\lambda = 1.5406$ Å). C, H, and N elemental analyses were performed on Vario EL III Elemental Analyzer.

X-ray crystallography: A single crystal of **4a-Pd** was mounted on a glass fiber for XRD analysis. Data were collected on a Rigaku AFC7R equipped with a graphite-monochromated $Mo_{K\alpha}$ radiation ($\lambda = 0.71073$ Å). Intensities were corrected for LP factors and empirical absorption by using the ψ scan technique. The structure was solved by direct methods and refined on F^2 by full-matrix least-squares techniques by using the Siemens SHELXTL version 5 package of crystallographic software.[32] All non-hydrogen atoms were refined anisotropically. The positions of H atoms were generated geometrically (C–H bond fixed at 0.96 Å) and allowed to ride on their parent carbon atoms before the final cycle of refinement. CCDC-851448 (**4a-Pd**) contains the supplementary crystallographic data for this paper. These data can be obtained free of charge from The Cambridge Crystallographic Data Centre via www.ccdc.cam.ac.uk/data_request/cif.

General procedures for the synthesis of 2a–2e: A slightly modified literature route was followed.[33] A mixture of 1-alkyl imidazole (25.0 mmol) and 3-bromopropyne (3.5 g, 29.0 mmol) in toluene (20 mL) was stirred for 30 min. at room temperature and then heated to reflux overnight. After removal of toluene, the residues were washed with Et_2O (3× 20 mL) and recrystallized from methanol/ether to give the resulting products.

1,2-Dimethyl-3-(prop-2-ynyl)-1*H*-imidazol-3-ium bromide (2a): White solid, yield: 80%. ^1H NMR ([D_6]DMSO): $\delta = 7.71$ (d, $J = 2.4$ Hz, 1H), 7.68 (d, $J = 2.4$ Hz, 1H), 5.20 (d, $J = 2.4$ Hz, 2H), 3.79 (s, 3H), 3.44 (s, 1H), 2.64 (s, 3H); ^{13}C NMR ([D_6]DMSO): $\delta = 145.2$, 123.0, 121.2, 78.9, 76.5, 38.0, 35.4, 10.0.

1-Methyl-3-(prop-2-ynyl)-1*H*-imidazol-3-ium bromide (2b):[33] Yellow solid, yield: 77%. ^1H NMR ([D_6]DMSO): $\delta = 9.27$ (s, 1H), 7.81 (s, 1H), 7.77 (s, 1H), 5.23 (d, $J = 2.8$ Hz, 2H), 3.89 (s, 3H), 3.83 (s, 1H); ^{13}C NMR ([D_6]DMSO): $\delta = 137.0$, 124.5, 122.6, 79.4, 76.6, 39.0, 36.7.

1-Butyl-2-methyl-3-(prop-2-ynyl)-1*H*-imidazol-3-ium bromide (2c): Yellow solid, yield: 84%. ^1H NMR ([D_6]DMSO): $\delta = 7.81$ (s, 2H), 5.23 (s, 2H), 4.17 (t, $J = 8$ Hz, 2H), 3.81 (s, 1H), 2.69 (s, 3H), 1.73–1.70 (m, 2H), 1.29–1.26 (m, 2H), 0.90 (t, $J = 8$ Hz, 3H); ^{13}C NMR ([D_6]DMSO): $\delta =$ 144.7, 122.0, 121.5, 79.0, 76.3, 48.0, 38.1, 31.6, 19.3, 13.9, 10.3.

1-Butyl-3-(prop-2-ynyl)-1*H*-imidazol-3-ium bromide (2d):[34] Yellow solid, yield: 80%. ^1H NMR ([D_6]DMSO): $\delta = 9.24$ (s, 1H), 7.86 (s, 1H), 7.78 (s, 1H), 5.21 (s, 2H), 4.22 (t, $J = 7.4$ Hz, 2H), 3.82 (s, 1H), 1.79 (t, $J = 7.5$ Hz, 2H), 1.26 (m, 2H), 0.90 (t, $J = 7.3$ Hz, 3H); ^{13}C NMR ([D_6]DMSO): $\delta = 136.5$, 123.3, 122.8, 79.4, 76.5, 49.3, 39.0, 31.7, 19.2, 13.7.

1-Mesityl-3-(prop-2-ynyl)-1*H*-imidazol-3-ium bromide (2e):[17b,23,34] Yellow solid, yield: 83%. ^1H NMR ([D_6]DMSO): $\delta = 9.55$ (s, 1H), 8.12 (s, 1H), 7.98 (s, 1H), 7.16 (s, 2H), 5.31 (s, 2H), 3.89 (s, 1H), 2.34 (s, 3H), 2.02 (s, 6H); ^{13}C NMR ([D_6]DMSO): $\delta = 140.8$, 138.0, 134.7, 131.6, 129.70, 124.7, 123.5, 79.8, 76.4, 21.0, 17.4, the $-CH_2-$ peak was covered by peaks of solvents.

General procedure for the synthesis of 3a–3i: These compounds were prepared according to slightly modified literature procedures.[17b] A mixture of benzyl bromide or *n*-butyl bromide (11.0 mmol) and NaN_3 (0.72 g, 11.0 mmol) in MeOH/H_2O (1:1, 30 mL) was heated to reflux for 2 h.

After cooling to room temperature, **2a–2e** (10.0 mmol), $CuSO_4 \cdot 5H_2O$ (0.37 g, 1.5 mmol) and sodium ascorbate (0.90 g, 4.5 mmol) were added, and the reaction mixture allowed to stir at ambient temperature for 24 h. The resulting solution was extracted with *n*-butyl alcohol (3×20 mL). The combined organic phase was washed with water and brine and dried over $MgSO_4$, concentrated under reduced pressure, and purified by flash chromatography on silica gel to give **3a–3i**.

1,2-Dimethyl-3-[(1-butyl-1*H*-1,2,3-triazol-4-yl)methyl]-1*H*-imidazol-3-ium bromide (3a): Yellow solid, yield: 56%. ^{1}H NMR (CD_3OD): δ=8.21 (s, 1H), 7.57 (s, 1H), 7.52 (s, 1H), 5.54 (s, 2H), 4.44 (t, J=7.2 Hz, 2H), 3.86 (s, 3H), 2.76 (s, 3H), 1.95–1.85 (m, 2H), 1.40–1.30 (m, 2H), 0.98 (t, J=7.2 Hz, 3H); ^{13}C NMR (CD_3OD): δ=145.1, 140.5, 124.1, 122.5, 120.9, 50.0, 42.7, 34.3, 31.9, 19.2, 12.4, 8.7.

1-[(1-Butyl-1*H*-1,2,3-triazol-4-yl)methyl]-3-methylimidazol-3-ium bromide (3b): Yellow solid, yield: 94%. ^{1}H NMR (CD_3OD): δ=9.14 (s, 1H), 8.30 (s, 1H), 7.72 (s, 1H), 7.65 (s, 1H), 5.63 (s, 2H), 4.47 (t, J=7.2 Hz, 2H), 3.99 (s, 3H), 1.95–1.87 (m, 2H), 1.39–1.34 (m, 2H), 0.98 (t, J=7.4 Hz, 3H); ^{13}C NMR (CD_3OD): δ=140.3, 136.8, 124.5, 123.9, 122.3, 50.0, 43.9, 35.4, 31.9, 19.3, 12.4.

1,2-Dimethyl-3-[(1-benzyl-1*H*-1,2,3-triazol-4-yl)methyl]-1*H*-imidazol-3-ium bromide (3c): Yellow solid, yield: 63%. ^{1}H NMR (CD_3OD): δ=8.22 (s, 1H), 7.56 (s, 1H), 7.55 (s, 1H), 7.40–7.30 (m, 5H), 5.63 (s, 2H), 5.52 (s, 2H), 3.84 (s, 3H), 2.74 (s, 3H); ^{13}C NMR (CD_3OD): δ=145.0, 140.9, 135.1, 128.7, 128.3, 127.91, 124.0, 122.5, 120.9, 53.7, 42.7, 34.2, 8.62.

1-[(1-Benzyl-1*H*-1,2,3-triazol-4-yl)methyl]-3-methylimidazol-3-ium bromide (3d): Yellow solid, yield: 87%. ^{1}H NMR ([D_6]DMSO): δ=9.22 (s, 1H), 8.34 (s, 1H), 7.76 (s, 1H), 7.70 (s, 1H), 7.38–7.33 (m, 5H), 5.63 (s, 2H), 5.54 (s, 2H), 3.86 (s, 3H). ^{13}C NMR ([D_6]DMSO): δ=141.2, 137.1, 136.1, 129.3, 128.8, 128.6, 125.1, 124.3, 122.8, 53.5, 44.0, 36.3.

1-Butyl-2-methyl-3-[(1-butyl-1*H*-1,2,3-triazol-4-yl)methyl]-1*H*-imidazol-3-ium bromide (3e): Brown oil, yield: 60%. ^{1}H NMR (CD_3OD): δ=8.28 (s, 1H), 7.62 (s, 2H), 5.57 (s, 2H), 4.45 (t, J=8 Hz, 2H), 4.22 (t, J=8 Hz, 2H), 2.82 (s, 3H), 1.96–1.80 (m, 4H), 1.45–1.30 (m, 4H), 1.05–0.95 (m, 6H); ^{13}C NMR (CD_3OD): δ=144.5, 140.4, 124.2, 121.4, 121.3, 49.9, 47.2, 42.8, 31.9, 31.3, 19.3, 19.2, 12.5, 12.4, 8.95.

1-Butyl-3-[(1-butyl-1*H*-1,2,3-triazol-4-yl)methyl]-1*H*-imidazol-3-ium bromide (3f): Brown oil, yield: 65%. ^{1}H NMR (CD_3OD): δ=9.20 (s, 1H), 8.27 (s, 1H), 7.71 (s, 2H), 5.61 (s, 2H), 4.46 (t, J=8 Hz, 2H), 4.28 (t, J=8 Hz, 2H), 1.96–1.85 (m, 4H), 1.45–1.30 (m, 4H), 1.05–0.95 (m, 6H); ^{13}C NMR (CD_3OD): δ=140.2, 136.1, 124.5, 122.6, 122.4, 49.9, 49.4, 43.8, 31.8, 31.7, 19.2, 19.1, 12.4, 12.3.

1-Butyl-3-[(1-phenyl-1*H*-1,2,3-triazol-4-yl)methyl]imidazol-3-ium bromide (3g): Brown solid, yield: 50%. ^{1}H NMR ([D_6]DMSO): δ=9.44 (s, 1H), 9.03 (s, 1H), 7.92–7.87 (m, 4H), 7.63 (t, J=8.2 Hz, 2H), 7.53 (t, J=7.2 Hz, 1H), 5.68 (s, 2H), 4.22 (t, J=7.24 Hz, 2H), 1.82–1.74 (m, 2H), 1.30–1.22 (m, 2H), 0.90 (t, J=7.2 Hz, 3H); ^{13}C NMR([D_6]DMSO): δ=142.0, 136.9, 136.8, 130.5, 129.5, 123.7, 123.2, 120.7, 49.2, 44.2, 31.78, 19.3, 13.7.

1-[(1-Benzyl-1*H*-1,2,3-triazol-4-yl)methyl]-3-butyl-1*H*-imidazol-3-ium bromide (3h):[34] Brown solid, yield: 91%. ^{1}H NMR ([D_6]DMSO): δ=9.31 (s, 1H), 8.34 (s, 1H), 7.78 (d, J=7.6 Hz, 2H,), 7.40–7.32 (m, 5H), 5.64 (s, 2H), 5.54 (s, 2H), 4.18 (t, J=7.2 Hz, 2H), 1.78–1.72 (m, 2H), 1.26–1.21 (m, 2H), 0.88 (t, J=7.2 Hz, 3H). ^{13}C NMR ([D_6]DMSO): δ=141.2, 136.6, 136.1, 129.3, 128.8, 128.5, 125.1, 123.1, 123.1, 53.5, 49.2, 44.1, 31.8, 19.2, 13.7.

1-[(1-Benzyl-1*H*-1,2,3-triazol-4-yl)methyl]-3-mesitylimidazol-3-ium bromide (3i): Brown solid, yield: 84%. ^{1}H NMR ([D_6]DMSO): δ=9.56 (s, 1H), 8.38 (s, 1H), 8.04 (s, 1H), 7.91 (s, 1H), 7.39–7.32 (m, 5H), 7.14 (s, 2H), 5.66 (d, J=3.6 Hz, 4H), 2.32 (s, 3H), 1.99 (s, 6H,); ^{13}C NMR ([D_6]DMSO): δ=141.1, 140.8, 138.2, 136.1, 134.7, 131.5, 129.7, 129.3, 128.8, 128.5, 125.1, 124.5, 123.7, 53.5, 44.7, 21.0, 17.3.

General procedure for the preparation of 4a–4n: KPF_6 (2.0 mmol) or $LiN(SO_2CF_3)_2$ (2.0 mmol) was added to a solution of **3a–3i** (1.0 mmol) in a mixture of water (5 mL) and acetone (5 mL) at room temperature. The resulting mixture was stirred at 25°C for 12 h. Acetone was removed under reduced pressure, and the water layer was extracted with ethyl acetate (3×10 mL). The combined organic layer was washed with water (3×10 mL) and evaporated to dryness in vacuo to give **4a–4n**.

1,2-Dimethyl-3-[(1-butyl-1*H*-1,2,3-triazol-4-yl)methyl]-1*H*-imidazol-3-ium hexafluorophosphate (4a): White solid, yield: 82%. ^{1}H NMR (CD_3OD): δ=8.06 (s, 1H), 7.46 (s, 1H), 7.42 (s, 1H), 5.47 (s, 2H), 4.40 (t, J=7.2 Hz, 2H), 3.82 (s, 3H), 2.70 (s, 3H), 1.90–1.83 (m, 2H), 1.35–1.29 (m, 2H), 0.94 (t, J=7.6 Hz, 3H); ^{13}C NMR (CD_3OD): δ=145.1, 140.5, 124.1, 122.4, 120.8, 49.9, 47.3, 42.7, 34.1, 31.7, 19.2, 12.4, 8.4; ^{31}P NMR (CD_3OD): δ=−144.6; ^{19}F NMR (CD_3OD): δ=−74.3 (d, J=706 Hz, 6F); IR (KBr, cm^{-1}): $\tilde{\nu}$ = 3165 (m), 2962 (m), 2875 (w), 1594 (m), 1541 (m), 1452 (m), 1392 (w), 1249 (s), 1140 (w), 1052 (m), 835 (vs), 791 (s), 762 (w), 741 (w), 559 (s); elemental analysis (%) calcd for $C_{12}H_{20}F_6N_5P$ (379.3): C 38.00, H 5.31, N 18.46; found C 38.12, H 5.25, N 18.39.

1-Methyl-3-[(1-butyl-1*H*-1,2,3-triazol-4-yl)methyl]-1*H*-imidazol-3-ium hexafluorophosphate (4b): Colorless oil, yield: 85%. ^{1}H NMR (CD_3OD): δ=8.88 (s, 1H), 8.11 (s, 1H), 7.61 (s, 1H), 7.55 (s, 1H), 5.53 (s, 2H), 4.43 (t, J=7.2 Hz, 2H), 3.93 (s, 3H), 1.92–1.82 (m, 2H), 1.40–1.30 (m, 2H), 0.96 (t, J=7.2 Hz, 3H); ^{13}C NMR (CD_3OD): δ=140.3, 136.7, 124.5, 123.8, 123.7,122.2, 122.1, 50.0, 43.7, 35.2, 31.7, 19.2, 12.3; ^{31}P NMR (CD_3OD): δ=−144.5; ^{19}F NMR (CD_3OD): δ=−73.7; IR (KBr, cm^{-1}): $\tilde{\nu}$ = 3164 (s), 2964 (s), 2877 (m), 2119 (w), 1575 (s), 1455 (m), 1385 (w), 1331 (w), 1228 (w), 1166 (s), 1055 (m), 839 (vs), 785 (m), 757 (m), 623 (m), 558 (s); elemental analysis (%) calcd for $C_{11}H_{18}F_6N_5P$ (365.3): C 36.17, H 4.97, N 19.17; found C 36.15, H 5.00, N 19.52.

1,2-Dimethyl-3-[(1-butyl-1*H*-1,2,3-triazol-4-yl)methyl)-1*H*-imidazol-3-ium bis(trifluoromethylsulfonyl)amide (4c): Colorless oil, yield: 85%. ^{1}H NMR (CD_3OD): δ=8.12 (s, 1H), 7.51 (s, 1H), 7.47 (s, 1H), 5.50 (s, 2H), 4.42 (t, J=6.8 Hz, 2H), 3.84 (s, 3H), 2.73 (s, 3H), 1.92–1.85 (m, 2H), 1.36–1.30 (m, 2H), 0.97 (t, J=7.2 Hz, 3H); ^{13}C NMR (CD_3OD): δ=145.1, 140.4, 123.9, 122.5, 120.8,, 49.9, 47.0, 42.7, 34.2, 31.8, 19.2, 12.3, 8.5; ^{19}F NMR (CD_3OD): δ=−80.6; IR (KBr, cm^{-1}): $\tilde{\nu}$ = 3150 (s), 2966 (s), 2879 (s), 2391 (w), 1592 (m), 1539 (m), 1456 (s), 1352 (vs), 1191 (vs), 1139 (vs), 1038 (vs), 946 (w), 835 (w), 789 (s), 763 (s), 741 (s), 655 (m), 616 (vs), 571 (s), 514 (s); elemental analysis (%) calcd for $C_{14}H_{20}F_6N_6O_4S_2$ (514.4): C 32.68, H 3.92, N 16.34; found C 32.62, H 3.90, N 16.37.

1-Methyl-3-[(1-butyl-1*H*-1,2,3-triazol-4-yl)methyl]-1*H*-imidazol-3-ium bis(trifluoromethylsulfonyl)amide (4d): Brown oil, yield: 90%. ^{1}H NMR (CD_3OD): δ=8.96 (s, 1H), 8.15 (s, 1H), 7.64 (s, 1H), 7.58 (s, 1H), 5.55 (s, 2H), 4.44 (t, J=7.2 Hz, 2H), 3.95 (s, 3H), 1.93–1.85 (m, 2H), 1.40–1.30 (m, 2H), 0.97 (t, J=7.6 Hz, 3H); ^{13}C NMR (CD_3OD): δ=140.2, 124.3, 123.8, 122.3, 121.4, 118.2, 50.0, 43.8, 35.2, 31.8, 19.2, 12.3; ^{19}F NMR (CD_3OD): δ=−80.6; IR (KBr, cm^{-1}): $\tilde{\nu}$ = 3156 (m), 2966 (m), 2879 (w), 2111 (w), 1575 (w), 1455 (w), 1353 (vs), 1595 (vs), 1138 (s), 1058 (vs), 842 (w), 788 (m), 741 (w), 617 (s), 571 (m), 514 (m); elemental analysis (%) calcd for $C_{13}H_{18}F_6N_6O_4S_2$ (500.4): C 31.20, H 3.63, N 16.79; found C 31.16, H 3.73, N 17.65.

1,2-Dimethyl-3-[(1-benzyl-1*H*-1,2,3-triazol-4-yl)methyl]-1*H*-imidazol-3-ium hexafluorophosphate (4e): Colorless solid, yield: 80%. ^{1}H NMR (CD_3OD): δ=8.10 (s, 1H), 7.47 (s, 1H), 7.43 (s, 1H), 7.40–7.30 (m, 5H), 5.60 (s, 2H), 5.46 (s, 2H), 3.81 (s, 3H), 2.70 (s, 3H); ^{13}C NMR (CD_3OD): δ=145.1, 140.9, 135.1, 128.7, 128.3, 127.9, 124.0, 122.5, 120.8, 53.7, 42.6, 34.1, 8.4; ^{31}P NMR: δ=−144.6; ^{19}F NMR (CD_3OD): δ=−74.3 (d, J=706 Hz, 6F); IR (KBr, cm^{-1}): $\tilde{\nu}$ = 3158 (s), 3090 (w), 3035 (w), 2964 (w), 1590 (m), 1537 (m), 1455 (m), 1371 (w), 1329 (w), 1125 (m), 1054 (m), 840 (vs), 748 (s), 722 (m), 559 (s); elemental analysis (%) calcd for $C_{15}H_{18}F_6N_5P$ (413.3): C 43.59, H 4.39, N 16.94, Found C 43.42, H 4.62, N 15.96.

1,2-Dimethyl-3-[(1-benzyl-1*H*-1,2,3-triazol-4-yl)methyl]-1*H*-imidazol-3-ium bis(trifluoromethylsulfonyl)amide (4f): Colorless oil, yield: 89%. ^{1}H NMR (CD_3OD): δ=8.12 (s, 1H), 7.50 (s, 1H), 7.45 (s, 1H), 7.40–7.30 (m, 5H), 5.61 (s, 2H), 5.48 (s, 2H), 3.82 (s, 3H), 2.72 (s, 3H); ^{13}C NMR (CD_3OD): δ=145.1, 141.0, 135.0, 128.7, 128.3, 127.8, 123.9, 122.5, 120.8, 53.8, 42.6, 34.1, 8.4; ^{19}F NMR (CD_3OD): δ=−80.6; IR (KBr, cm^{-1}): $\tilde{\nu}$ = 3150 (s), 3094 (w), 3027 (w), 2964 (w), 2390 (vw), 1592 (m), 1539 (m), 1498 (w), 1456 (m), 1352 (vs), 1195 (vs), 1139 (vs), 1056 (vs), 798 (m), 741 (s), 654 (m), 616 (s), 671 (s), 514 (s), 464 (vw); elemental analysis

(%) calcd for $C_{17}H_{18}F_6N_6O_4S_2$ (548.5): C 37.23, H 3.31, N 15.32; found C 37.17, H 3.30, N 15.84.

1-Methyl-3-[(1-benzyl-1*H*-1,2,3-triazol-4-yl)methyl]-1*H*-imidazol-3-ium hexafluorophosphate (4g): White solid, yield: 90%. ^{1}H NMR (CD_3OD): $\delta=8.91$ (s, 1H), 8.13 (s, 1H), 7.60 (s, 1H), 7.54 (s, 1H), 7.38–7.33 (m, 5H), 5.61 (s, 2H), 5.51 (s, 2H), 3.92 (s, 3H). ^{13}C NMR (CD_3OD): $\delta=$ 140.6, 136.8, 135.0, 128.7, 128.3, 128.0, 124.4, 123.8, 122.2, 53.8, 43.7, 35.2; ^{31}P NMR: $\delta=-144.5$; ^{19}F NMR (CD_3OD): $\delta=-74.2$ (d, $J=706$ Hz, 6F); IR (KBr, cm^{-1}): $\tilde{\nu}=$ 3160 (m), 3112 (m), 2967 (vw), 2872 (w), 1564 (m), 1445 (m), 1428 (w), 1322 (m), 1228 (m), 1163 (s), 1055 (m), 841 (vs), 742 (m), 624 (w), 716 (m), 558 (s); elemental analysis (%) calcd for $C_{14}H_{16}F_6N_5P$ (399.3): C 42.11, H 4.04, N 17.54; found C 42.52, H 4.58, N 17.31.

1-Butyl-3-[(1-benzyl-1*H*-1,2,3-triazol-4-yl)methyl]-1*H*-imidazol-3-ium hexafluorophosphate (4h): Brown solid, yield: 82%. ^{1}H NMR (CD_3OD): $\delta=9.00$ (s, 1H), 8.14 (s, 1H), 7.63 (d, $J=2.4$ Hz, 2H), 7.40–7.32 (m, 5H), 5.62 (s, 2H), 5.51 (s, 2H), 4.21 (t, $J=7.6$ Hz, 2H), 1.90–1.80 (m, 2H), 1.40–1.31 (m, 2H), 0.98 (t, $J=7.2$ Hz, 3H); ^{13}C NMR (CD_3OD): $\delta=$ 135.0, 128.7, 128.3, 128.0, 124.5, 122.6, 122.6, 122.4, 122.3, 53.8, 49.4, 43.7, 31.5, 19.0, 12.3; ^{31}P NMR (CD_3OD): $\delta=-144.5$; ^{19}F NMR (CD_3OD): $\delta=$ -74.2 (d, $J=708$ Hz, 6F); IR (KBr, cm^{-1}): $\tilde{\nu}=$ 3163 (s), 3112 (m), 2962 (m), 2872 (w), 1569 (m), 1455 (m), 1363 (w), 1334 (w), 1223 (w), 1165 (s), 1126 (w), 1056 (w), 836 (vs), 741 (s), 716 (m), 632 (w), 558 (s), 471 (vs); elemental analysis (%) calcd for $C_{17}H_{22}F_6N_5P$ (441.4): C 46.26, H 5.02, N 15.87; found C 46.20, H 4.98, N 15.74.

1-Butyl-3-[(1-benzyl-1*H*-1,2,3-triazol-4-yl)methyl]-1*H*-imidazol-3-ium bis(trifluoromethylsulfonyl)amide (4i): Brown oil, yield: 91%. ^{1}H NMR (CD_3OD): $\delta=9.03$ (s, 1H), 8.15 (s, 1H), 7.63 (d, $J=2.4$ Hz, 2H), 7.40–7.32 (m, 5H), 5.62 (s, 2H), 5.53 (s, 2H), 4.22 (t, $J=7.2$ Hz, 2H), 1.90–1.80 (m, 2H), 1.40–1.32 (m, 2H), 0.98 (t, $J=7.2$ Hz, 3H); ^{13}C NMR (CD_3OD): $\delta=136.0$, 135.0, 128.7, 128.4, 127.9, 124.6, 122.7, 122.4, 121.4, 118.2, 53.8, 49.4, 43.8, 31.6, 19.0, 12.3; ^{19}F NMR (CD_3OD): $\delta=-80.6$; IR (KBr, cm^{-1}): $\tilde{\nu}=$ 3149 (m), 2966 (m), 2879 (w), 1565 (m), 1457 (m), 1352 (vs), 1195 (vs), 1136 (s), 1157 (vs), 790 (w), 740 (m), 616 (s), 571 (m), 513 (m); elemental analysis (%) calcd for $C_{19}H_{22}F_6N_6O_4S_2$ (576.5): C 39.58, H 3.85, N 14.58; found C 39.43, H 4.22, N 14.46.

1-Butyl-3-[(1-phenyl-1*H*-1,2,3-triazol-4-yl)methyl]-1*H*-imidazol-3-ium hexafluorophosphate (4j): Brown solid, yield: 75%. ^{1}H NMR ([D$_6$]acetone): $\delta=9.19$ (s, 1H), 8.76 (s, 1H), 7.95–7.80 (m, 4H), 7.70–7.50 (m, 3H), 5.79 (s, 2H), 4.41 (t, $J=7.2$ Hz, 2H), 2.00–1.90 (m, 2H), 1.45–1.35(m, 2H), 0.95 (t, $J=7.2$ Hz, 3H); ^{13}C NMR ([D$_6$]acetone): $\delta=141.3$, 136.2, 129.9, 129.0, 122.9, 122.8, 120.4, 49.6, 44.3, 31.8, 19.1, 12.8; ^{31}P NMR: $\delta=-144.2$; ^{19}F NMR ([D$_6$]acetone): $\delta=-72.3$; IR (KBr, cm^{-1}): $\tilde{\nu}=$ 3164 (m), 3120 (w), 2972 (m), 2879 (w), 1597 (m), 1569 (m), 1503 (m), 1456 (m), 1338 (vw), 1242 (m), 1171 (s), 1109 (vw), 1049 (s), 851 (vs), 755 (m), 688 (w), 636 (w), 558 (s), 571 (w); elemental analysis (%) calcd for $C_{16}H_{20}F_6N_5P$ (427.3): C 44.97, H 4.72, N 16.39; found C 44.74, H 5.07, N 16.21.

1-Butyl-3-[(1-phenyl-1*H*-1,2,3-triazol-4-yl)methyl)-1*H*-imidazol-3-ium bis(trifluoromethylsulfonyl)amide (4k): Colorless oil, yield: 81%. ^{1}H NMR (CD_3OD): $\delta=9.05$ (s, 1H), 8.64 (s, 1H), 7.82 (s, 2H), 7.70–7.50 (m, 5H), 5.64 (s, 2H), 4.24 (t, $J=7.6$ Hz, 2H), 1.93–1.85 (m, 2H), 1.42–1.36(m, 2H), 0.98 (t, $J=7.6$ Hz, 3H); ^{13}C NMR (CD_3OD): $\delta=141.0$, 136.7, 136.0, 129.6, 129.0, 122.7, 121.4, 120.4, 118.2, 49.5, 43.8, 31.6, 19.0, 12.3; ^{19}F NMR (CD_3OD): $\delta=-80.6$; IR (KBr, cm^{-1}): $\tilde{\nu}=$ 3151 (s), 3115 (m), 2967 (m), 2936 (m), 2879 (w), 2390 (vw), 1599 (m), 1564 (m), 1505 (s), 1468 (m), 1363 (w), 1352 (vs), 1195 (vs), 1137 (vs), 1056 (vs), 993 (w), 914 (vw), 843 (w), 762 (s), 692 (m), 654 (m), 616 (s), 571 (s), 513 (m); elemental analysis (%) calcd for $C_{18}H_{20}F_6N_6O_4S_2$ (562.5): C 38.43, H 3.58, N 14.94; found C 38.42, H 4.04, N 15.00.

1-Butyl-3-[(1-butyl-1*H*-1,2,3-triazol-4-yl)methyl]-1*H*-imidazol-3-ium hexafluorophosphate (4l): Colorless oil, yield: 82%.^{1}H NMR ([D$_6$]acetone): $\delta=9.10$ (s, 1H), 8.18 (s, 1H), 7.77 (s, 2H), 5.66 (s, 2H), 4.45 (t, $J=$ 6.8 Hz, 2H), 4.38 (t, $J=6.8$ Hz, 2H), 2.00–1.85 (m, 4H), 1.40–1.25 (m, 4H), 1.00–0.85 (m, 6H); ^{13}C NMR ([D$_6$]acetone): $\delta=140.1$, 136.0, 124.2, 122.8, 122.7, 49.7, 49.6, 44.3, 32.0, 31.8, 19.3, 19.1, 12.8, 12.7; ^{31}P NMR ([D$_6$]acetone): $\delta=-144.2$; ^{19}F NMR ([D$_6$]acetone): $\delta=-72.2$ (d, $J=$ 706 Hz, 6F); IR (KBr, cm^{-1}): $\tilde{\nu}=$ 3159 (m), 2964 (s), 2877 (m), 1567 (m), 1464 (m), 1326 (w), 1228 (w), 1161 (s), 1054 (m), 840 (vs), 757 (w), 629 (w), 558 (s); elemental analysis (%) calcd for $C_{14}H_{24}F_6N_5P$ (407.3): C 41.28, H 5.94, N 17.19; found C 40.93, H 5.80, N 16.89.

1-Butyl-3-[(1-butyl-1*H*-1,2,3-triazol-4-yl)methyl]-2-methyl-1*H*-imidazol-3-ium hexafluorophosphate (4m): Colorless oil, yield: 90%.^{1}H NMR([D$_6$]acetone): $\delta=8.17$ (s, 1H), 7.65 (s, 2H), 5.60 (s, 2H), 4.44 (t, $J=7.2$ Hz, 2H), 4.31 (t, $J=7.2$ Hz, 2H), 1.95–1.80 (m, 4H), 1.45–1.30 (m, 4H), 1.00–0.90 (m, 6H). ^{13}C NMR ([D$_6$]acetone): $\delta=144.7$, 140.4, 123.8, 121.5, 121.4, 49.7, 48.1, 43.1, 32.0, 31.5, 19.3, 19.2, 12.8, 12.8, 9.25; ^{31}P NMR ([D$_6$]acetone): $\delta=-144.3$; ^{19}F NMR ([D$_6$]acetone): $\delta=$ -72.5 (d, $J=706$ Hz, 6F); IR (KBr, cm^{-1}): $\tilde{\nu}=$ 3658 (w), 3448 (w), 3156 (s), 2964 (s), 2878 (s), 1588 (m), 1532 (m), 1470 (s), 1338 (w), 1263 (w), 1226 (w), 1154 (m), 1054 (s), 840 (vs), 762 (s), 667 (vw), 558 (s), 484 (vw); elemental analysis (%) calcd for $C_{15}H_{26}F_6N_5P\cdot H_2O$ (439.4): C 41.00, H 6.42, N 15.94; found C 40.87, H 6.78, N 16.35.

1-Mesityl-3-[(1-benzyl-1*H*-1,2,3-triazol-4-yl)methyl]-1*H*-imidazol-3-ium hexafluorophosphate (4n): Brown solid, yield: 91%. ^{1}H NMR (CD_3OD): $\delta=9.22$ (s, 1H), 8.19 (s, 1H), 7.88 (s, 1H), 7.70 (s, 1H), 7.40–7.30 (m, 5H), 7.13 (s, 2H), 5.67 (s, 2H), 5.65 (s, 2H), 2.37 (s, 3H), 2.06 (s, 6H,); ^{13}C NMR (CD_3OD): $\delta=141.2$, 137.5, 135.0, 134.4, 129.3, 128.7, 128.4, 127.9, 124.5, 124.4, 123.1, 53.8, 44.2, 19.7, 15.8; ^{31}P NMR: $\delta=-144.6$; ^{19}F NMR (CD_3OD): $\delta=-74.5$ (d, $J=706$ Hz, 6F); IR (KBr, cm^{-1}): $\tilde{\nu}=$ 3443 (w), 3156 (m), 3035 (w), 2925 (w),1609 (w), 1552 (m), 1456 (w), 1486 (m), 1331 (vw), 1201 (s), 1161 (m), 1054 (w), 841 (vs), 774 (vw), 739 (s), 670 (w), 623 (vw), 558 (s); elemental analysis (%) calcd for $C_{22}H_{24}F_6N_5P$ (503.4): C 52.49, H 4.81, N 13.91; found C 52.35, H 5.19, N 13.77.

Synthesis of Pd-4a: $PdCl_2$ (0.035 g, 0.2 mmol) was added to a stirred acetone solution (10 mL) of **4a** (0.152 g, 0.4 mmol). The resulting mixture was stirred for 12 h at 60°C. After cooling to room temperature, the solvent was removed under reduced pressure to a give pale yellow solid in quantitative yield. Slow evaporation of an acetone solution of **4a-Pd** gave single crystals suitable for X-ray diffraction. ^{1}H NMR ([D$_6$]acetone): $\delta=8.57$ (s, 2H), 7.87 (d, $J=2$ Hz, 2H), 7.72 (d, $J=2$ Hz, 2H), 6.03 (s, 4H), 4.68 (t, $J=8$ Hz, 4H), 4.00 (s, 6H), 3.10 (s, 6H), 2.03–1.96 (m, 4H), 1.44–1.34 (m, 4H), 0.97 (t, $J=8$ Hz, 6H); ^{13}C NMR ([D$_6$]acetone): $\delta=$ 145.8, 141.6, 127.6, 123.3, 122.2, 52.0, 42.7, 34.9, 31.5, 19.1, 12.8, 10.3; ^{31}P NMR: $\delta=-144.3$; ^{19}F NMR ([D$_6$]acetone): $\delta=-72.6$ (d, $J=714$ Hz, 12F); IR (KBr, cm^{-1}): $\tilde{\nu}=$ 3435 (m), 3159 (m), 2960 (m), 2876 (w), 1597 (m), 1540 (m),1541 (m), 1538 (m), 1264 (m), 1160 (m), 1113 (m), 1050 (w), 840 (vs), 749 (m), 646 (vw), 559 (s); elemental analysis (%) calcd for $C_{24}H_{40}C_{12}F_{12}N_{10}P_2Pd$ (935.9): C 30.80, H 4.31, N 14.97; ound C 31.06, H 4.05, N 15.11.

General procedure for Suzuki–Miyaura cross-coupling reactions in 4a: $PdCl_2$ (1.8 mg, 0.01 mmol) was added to a solution of **4a** (2.0 g, 2.6 mmol) in acetone (5.0 mL), which was then stirred at 60°C for 6 h. After removal of acetone in vacuo, aryl halide (0.5 mmol), aryl boronic acid (0.6 mmol), K_2CO_3 (0.14 g, 1.0 mmol), and water (0.5 mL) were added. The resulting mixture was stirred at 100°C for 5 h. After cooling to ambient temperature, the product was extracted with diethyl ether (3× 5 mL). The combined organic layer was concentrated under reduced pressure and was purified by short-path silica-gel column chromatography to give the target product. The identities of the products were confirmed by comparison with literature spectroscopic data. The resulting catalytic solution containing palladium species was washed with water (3×5 mL) to remove inorganic salts and then dried in vacuo at 60°C for 4 h to remove traces of water and employed for the next cycle.

Synthesis of Pd-Suzuki: After the first run of the coupling reaction between iodobenzene and phenylboronic acid, ethanol (5 mL) was added to the resulting mixture, and the resulting black powder was isolated by centrifugation, washed with ethanol (3 mL), and then centrifuged. This process was repeated three times. The sample for TEM analysis was prepared by ultrasonication of the black powder in ethanol and directly dropping the dispersion onto a carbon-coated copper grid. The sample for XPS analysis was prepared by drying the black powder under reduced pressure.

Synthesis of Pd-NaBH$_4$: $PdCl_2$ (3.6 mg, 0.02 mmol) was added to a solution of **4a** (1.0 g, 2.6 mmol) in THF (10 mL) and the mixture stirred at

60 °C for 12 h. After cooling to ambient temperature, 0.1 M aqueous $NaBH_4$ solution (0.4 mL) was quickly added to the stirred solution, which was then stirred for 0.5 hour. A black powder was isolated by centrifugation. The powder was washed with ethanol (3 mL) and centrifuged, and this process was repeated three times. The sample for TEM was prepared by ultrasonication of the powder in ethanol and directly dropping the resulting dispersion onto a carbon-coated copper grid. The sample for XRD and XPS analyses were prepared by drying the isolated black powder under reduced pressure.

Acknowledgements

This work was financially supported by 973 Program (2010CB933501, 2011CBA00502), Natural Science Foundation of China (20971122), and "One Hundred Talent Project" of Chinese Academy of Sciences.

[1] a) F. Bellina, R. Rossi, *Chem. Rev.* **2010**, *110*, 1082–1146; b) A. Brennführer, H. Neumann, M. Beller, *Angew. Chem.* **2009**, *121*, 4176–4196; *Angew. Chem. Int. Ed.* **2009**, *48*, 4114–4133; c) M. N. Birkholz, Z. Freixab, P. W. N. M. van Leeuwen, *Chem. Soc. Rev.* **2009**, *38*, 1099–1118; d) D. Enders, T. Balensiefer, *Acc. Chem. Res.* **2004**, *37*, 534–541; e) P. L. Arnold, S. Pearson, *Coord. Chem. Rev.* **2007**, *251*, 596–609.

[2] a) F. Bellinaa, R. Rossi, *Adv. Synth. Catal.* **2010**, *352*, 1223–1276; b) P. V. Sashuk, D. Schoeps, H. Plenio, *Chem. Commun.* **2009**, 770–771; c) D. Meyer, M. A. Taige, A. Zeller, K. Hohlfeld, S. Ahrens, T. Strassne, *Organometallics* **2009**, *28*, 2142–2149; d) F. E. Hahn, M. C. Jahnke, *Angew. Chem.* **2008**, *120*, 3166–3216; *Angew. Chem. Int. Ed.* **2008**, *47*, 3122–3172; e) D. J. M. Snelders, R. Kreiter, J. Firet, G. van Koten, R. J. M. K. Gebbink, *Adv. Synth. Catal.* **2008**, *350*, 262–266.

[3] a) M. Lamblin, L. Nassar-Hardy, J. C. Hierso, E. Fouquet, F. X. Felpinb, *Adv. Synth. Catal.* **2010**, *352*, 33–79; b) J. Durand, E. Teuma, M. Gómez, *Eur. J. Inorg. Chem.* **2008**, 3577–3586; c) A. Corma, H. García, *Chem. Rev.* **2008**, *108*, 2096–2126; d) D. Astruc, F. Lu, J. R. Aranzaes, *Angew. Chem.* **2005**, *117*, 8062–8083; *Angew. Chem. Int. Ed.* **2005**, *44*, 7852–7872; e) M. Moreno-Mañas, R. Pleixats, *Acc. Chem. Res.* **2003**, *36*, 638–643.

[4] a) R. Liu, C. Wu, Q. Wang, J. Ming, Y. Hao, Y. Yu, F. Zhao, *Green Chem.* **2009**, *11*, 979–985; b) C. Ornelas, L. Salmon, J. R. Aranzaes, D. Astruc, *Chem. Commun.* **2007**, 4946–4948; c) T. R. Hendricks, E. E. Dams, S. T. Wensing, I. Lee, *Langmuir* **2007**, *23*, 7404–7410; d) Z. Hou, N. Theyssen, W. Leitner, *Green Chem.* **2007**, *9*, 127–132; e) L. S. Ott, R. G. Finke, *Inorg. Chem.* **2006**, *45*, 8382–8393.

[5] a) L. M. Rossi, I. M. Nangoi, N. J. S. Costa, *Inorg. Chem.* **2009**, *48*, 4640–4642; b) J. N. Park, A. J. Forman, W. Tang, J. Cheng, Y. S. Hu, H. Lin, E. W. McFarland, *Small* **2008**, *4*, 1694–1697; c) B. M. Choudary, S. Madhi, N. S. Chowdari, M. L. Kantam, B. Sreedhar, *J. Am. Chem. Soc.* **2002**, *124*, 14127–14136; d) S. H. Li, J. H. Wang, Y. L. Kou, S. B. Zhang, *Chem. Eur. J.* **2010**, *16*, 1812–1818.

[6] a) J. Dupont, J. D. Scholten, *Chem. Soc. Rev.* **2010**, *39*, 1780–1804; b) N. Yan, C. Xiao, Y. Kou, *Coord. Chem. Rev.* **2010**, *254*, 1179–1218; c) Y. Tsuji, T. Fujihara, *Inorg. Chem.* **2007**, *46*, 1895–1902; d) X. Huang, Y. P. Wang, X. P. Liao, B. Shi, *Chem. Commun.* **2009**, 4687–4689.

[7] a) B. Feng, Z. Hou, H. Yang, X. Wang, Y. Hu, H. Li, Y. Qiao, X. Zhao, Q. Huang, *Langmuir* **2010**, *26*, 2505–2513; b) N. Mejías, R. Pleixats, A. Shafir, M. Medio-Simón, G. Asensio, *Eur. J. Org. Chem.* **2010**, 5090–5099; c) D. Saha, K. Chattopadhyay, B. C. Ranu, *Tetrahedron Lett.* **2009**, *50*, 1003–1006.

[8] a) C. C. Luo, Y. H. Zhang, Y. G. Wang, *J. Mol. Catal. A* **2005**, *229*, 7–12; b) W. Han, C. Liu, Z. L. Jin, *Org. Lett.* **2007**, *9*, 4005–4007; c) L. K. Yeung, R. M. Crooks, *Nano Lett.* **2001**, *1*, 14–17.

[9] a) T. Welton, *Chem. Rev.* **1999**, *99*, 2071–2083; b) R. Sheldon, *Chem. Commun.* **2001**, 2399–2407; c) J. S. Wilkes, *J. Mol. Catal. A* **2004**, *214*, 11–17; d) T. L. Greaves, C. J. Drummond, *Chem. Rev.* **2008**, *108*, 206–237; e) M. Smiglak, A. Metlen, R. D. Rogers, *Acc. Chem. Res.* **2007**, *40*, 1182–1192; f) N. Jain, A. Kumar, S. Chauhan, S. M. S. Chauhan, *Tetrahedron* **2005**, *61*, 1015–1060; g) B. Wu, W. W. Liu, Y. M. Zhang, H. P. Wang, *Chem. Eur. J.* **2009**, *15*, 1804–1810.

[10] a) N. Yan, Y. Yuan, P. J. Dyson, *Chem. Commun.* **2011**, *47*, 2529–2531; b) F. Bellina, A. Bertoli, B. Melai, F. Scalesse, F. Signori, C. Chiappe, *Green Chem.* **2009**, *11*, 622–629; c) B. Léger, A. Denicourt-Nowicki, H. Olivier-Bourbigou, A. Roucoux, *Tetrahedron Lett.* **2009**, *50*, 6531–6533; d) X. Yang, N. Yan, Z. Fei, R. M. Crespo-Quesada, G. Laurenczy, L. Kiwi-Minsker, Y. Kou, Y. Li, P. J. Dyson, *Inorg. Chem.* **2008**, *47*, 7444–7446; e) Z. F. Fei, T. J. Geldbach, D. B. Zhao, P. J. Dyson, *Chem. Eur. J.* **2006**, *12*, 2122–2130; f) V. Calò, A. Nacci, A. Monopoli, P. Cotugno, *Chem. Eur. J.* **2009**, *15*, 1272–1279.

[11] a) C. Fliedel, G. Schnee, P. Braunstein, *Dalton Trans.* **2009**, 2474–2476; b) H. Itoh, K. Naka, Y. Chujo, *J. Am. Chem. Soc.* **2004**, *126*, 3026–3027; c) K. S. Kim, D. Demberelnyamba, H. Lee, *Langmuir* **2004**, *20*, 556–560.

[12] a) D. Zhao, Z. Fei, T. J. Geldbach, R. Scopelliti, P. Dyson, *J. Am. Chem. Soc.* **2004**, *126*, 15876–15882; b) D. Zhao, Z. Fei, R. Scopelliti, P. J. Dyson, *Inorg. Chem.* **2004**, *43*, 2197–2205; c) F. Mazille, Z. Fei, D. Kuang, D. Zhao, S. M. Zakeeruddin, M. Gratzel, P. J. Dyson, *Inorg. Chem.* **2006**, *45*, 1585–1590.

[13] a) R. Wang, M. M. Piekarski, J. M. Shreeve, *Org. Biomol. Chem.* **2006**, *4*, 1878–1886; b) R. Wang, Z. Zeng, B. Twamley, M. M. Piekarski, J. M. Shreeve, *Eur. J. Org. Chem.* **2007**, 655–661.

[14] a) Y. Hu, Y. Y. Yu, Z. S. Hou, H. Li, X. G. Zhao, B. Fenga, *Adv. Synth. Catal.* **2008**, *350*, 2077–2085; b) R. R. Dykeman, N. Yan, R. Scopelliti, P. J. Dyson, *Inorg. Chem.* **2011**, *50*, 717–719.

[15] a) J. C. Xiao, B. Twamley, J. M. Shreeve, *Org. Lett.* **2004**, *6*, 3845–3847; b) J. C. Xiao, J. M. Shreeve, *J. Org. Chem.* **2005**, *70*, 3072–3078; c) C. M. Jin, B. Twamley, J. M. Shreeve, *Organometallics* **2005**, *24*, 3020–3023.

[16] a) Y. Li, M. A. El-Sayed, *J. Phys. Chem. B* **2001**, *105*, 8938–8943; b) D. Zhao, M. Wu, Y. Kou, E. Min, *Catal. Today* **2002**, *74*, 157–189; c) A. Roucoux, J. Schulz, H. Patin, *Adv. Synth. Catal.* **2003**, *345*, 222–229; d) Y. B. Liu, C. Khemtong, J. Hu, *Chem. Commun.* **2004**, 398–399; e) C. A. Stowell, B. A. Korgel, *Nano Lett.* **2005**, *5*, 1203–1207.

[17] a) V. V. Rostovtsev, L. G. Green, V. V. Fokin, K. B. Sharpless, *Angew. Chem.* **2002**, *114*, 2708–2711; *Angew. Chem. Int. Ed.* **2002**, *41*, 2596–2599; b) K. Zeitler, I. Mager, *Adv. Synth. Catal.* **2007**, *349*, 1851–1857; c) M. Meise, R. Haag, *ChemSusChem* **2008**, *1*, 637–642.

[18] a) F. Santoyo-Gonzalez, F. Hernandez-Mateo, *Chem. Soc. Rev.* **2009**, *38*, 3449–3462; b) Z. Kaleta, O. Egyed, T. Soos, *Org. Biomol. Chem.* **2005**, *3*, 2228–2230; c) A. Bastero, D. Font, M. A. Pericás, *J. Org. Chem.* **2007**, *72*, 2460–2468; d) M. Janssen, C. Müller, D. Vogt, *Adv. Synth. Catal.* **2009**, *351*, 313–318; e) S. M. Lee, H. Chen, T. V. O'Halloran, S. T. Nguyen, *J. Am. Chem. Soc.* **2009**, *131*, 9311–9320.

[19] a) H. Struthers, T. L. Mindt, R. Schibli, *Dalton Trans.* **2010**, *39*, 675–696; b) D. Schweinfurth, R. Pattacini, S. Strobel, B. Sarkar, *Dalton Trans.* **2009**, 9291–9297; c) L. Ackermann, H. K. Potukuchi, D. Landsberg, R. Vicente, *Org. Lett.* **2008**, *10*, 3081–3084.

[20] a) C. Ornelas, A. K. Diallo, J. Ruiz, D. Astruc, *Adv. Synth. Catal.* **2009**, *351*, 2147–2154; b) C. Ornelas, J. Ruiz, L. Salmon, D. Astruc, *Adv. Synth. Catal.* **2008**, *350*, 837–845; c) N. T. S. Phan, M. V. D. Sluys, C. W. Jones, *Adv. Synth. Catal.* **2006**, *348*, 609–679.

[21] R. J. Detz, S. A. Heras, R. de Gelder, P. W. N. M. van Leeuwen, H. Hiemstra, J. N. H. Reek, J. H. van Maarseveen, *Org. Lett.* **2006**, *8*, 3227–3230.

[22] a) D. Liu, W. Gao, Q. Dai, X. Zhang, *Org. Lett.* **2005**, *7*, 4907–4910; b) Q. Dai, W. Gao, D. Liu, L. M. Kapes, X. Zhang, *J. Org. Chem.* **2006**, *71*, 3928–3934.

[23] S. Warsink, R. M. Drost, M. Lutz, A. L. Spek, C. J. Elsevier, *Organometallics* **2010**, *29*, 3109–3116.

[24] a) E. M. Schuster, G. Nisnevich, M. Botoshansky, M. Gandelman, *Organometallics* **2009**, *28*, 5025–5031; b) E. M. Schuster, M. Botoshansky, M. Gandelman, *Organometallics* **2009**, *28*, 7001–7005.

[25] a) C. Zhou, J. Wang, L. Li, R. Wang, M. Hong, *Green Chem.* **2011**, *13*, 2100–2106; b) L. Li, J. Wang, C. Zhou, R. Wang, M. Hong, *Green Chem.* **2011**, *13*, 2071–2077.
[26] S. Ahrens, A. Peritz, T. Strassner, *Angew. Chem.* **2009**, *121*, 8048–8051; *Angew. Chem. Int. Ed.* **2009**, *48*, 7908–7910.
[27] Gaussian 03, revision D.02; Gaussian, Inc.: Wallingford CT, **2004**.
[28] B. Hu, T. Wu, K. Ding, X. Zhou, T. Jiang, B. Han, *J. Phys. Chem. C* **2010**, *114*, 3396–3400.
[29] A. Kern, W. Eysel, Mineralogisch-Petrograph. Inst. Univ. Heidelberg, Germany. ICDD Grant-in-Aid, **1993**.
[30] a) S. Eyley, W. Thielemans, *Chem. Commun.* **2011**, *47*, 4177–4179; b) V. Lockett, R. Sedev, C. Bassell, J. Ralston, *Phys. Chem. Chem. Phys.* **2008**, *10*, 1330–1335.
[31] A. Devadoss, C. E. D. Chidsey, *J. Am. Chem. Soc.* **2007**, *129*, 5370–5371.
[32] G. M. Sheldrick SHELXTL-97, Program for the Solution of Crystal Structures, University of Göttingen: Germany **1997**.
[33] Y. Gao, H. X. Gao, C. Piekarski, J. M. Shreeve, *Eur. J. Inorg. Chem.* **2007**, 4965–4972.
[34] S. Gu, H. Xu, N. Zhang, W. Chen, *Chem. Asian J.* **2010**, *5*, 1677–1686.

Received: November 18, 2011
Revised: March 3, 2012
Published online: May 15, 2012

